BBA - Proteins and Proteomics 1868 (2020) 140298

Contents lists available at ScienceDirect

BBA - Proteins and Proteomics

journal homepage: www.elsevier.com/locate/bbapap

Molecular characterization of an aggregation-prone variant of alpha-synuclein used to model synucleinopathies

Caterina Masaracchia[a,1], Annekatrin König[a,1], Ariel A. Valiente-Gabioud[b], Pablo Peralta[b], Filippo Favretto[c], Timo Strohäker[d], Diana F. Lázaro[a], Markus Zweckstetter[c,d,e], Claudio O. Fernandez[b], Tiago F. Outeiro[a,f,g,*]

[a] Department of Experimental Neurodegeneration, Center for Nanoscale Microscopy and Molecular Physiology of the Brain, Center for Biostructural Imaging of Neurodegeneration, University Medical Center Göttingen, Göttingen, Germany
[b] Max Planck Laboratory for Structural Biology, Chemistry and Molecular Biophysics of Rosario (MPLbioR, UNR-MPIbpC) and Instituto de Investigaciones para el Descubrimiento de Fármacos de Rosario (IIDEFAR, UNR-CONICET), Universidad Nacional de Rosario, Ocampo y Esmeralda, S2002LRK Rosario, Argentina
[c] German Center for Neurodegenerative Diseases (DZNE), Von-Siebold-Str. 3a, 37075 Göttingen, Germany
[d] Department of Neurology, University Medical Center Göttingen, University of Göttingen, Waldweg 33, 37073 Göttingen, Germany
[e] Department for NMR-based Structural Biology, Max Planck Institute for Biophysical Chemistry, Am Fassberg 11, 37077 Göttingen, Germany
[f] Max Planck Institute for Experimental Medicine, Göttingen, Germany
[g] Institute of Neuroscience, Medical School, Newcastle University, Framlington Place, Newcastle Upon Tyne NE2 4HH, UK

ARTICLE INFO

Keywords:
Alpha-synuclein
Parkinson's disease
Neurodegeneration
Protein aggregation
Misfolding

ABSTRACT

The misfolding and aggregation of alpha-synuclein (aSyn) are thought to be central events in synucleinopathies. The physiological function of aSyn has been related to vesicle binding and trafficking, but the precise molecular mechanisms leading to aSyn pathogenicity are still obscure. In cell models, aSyn does not readily aggregate, even upon overexpression. Therefore, cellular models that enable the study of aSyn aggregation are essential tools for our understanding of the molecular mechanisms that govern such processes. Here, we investigated the structural features of SynT, an artificial variant of aSyn that has been widely used as a model of aggregation in mammalian cell systems, since it is more prone to aggregation than aSyn. Using Nuclear Magnetic Resonance (NMR) spectroscopy we performed a detailed structural characterization of SynT through a systematic comparison with normal, unmodified aSyn. Interestingly, we found that the conformations adopted by SynT resemble those described for the unmodified protein, demonstrating the usefulness of SynT as a model for aSyn aggregation. However, subtle differences were observed at the N-terminal region involving transient intra and/or intermolecular interactions that are known to regulate aSyn aggregation. Importantly, our results indicate that disturbances in the N-terminal region of SynT, and the consequent decrease in membrane binding of the modified protein, might contribute to the observed aggregation behavior of aSyn, and validate the use of SynT, one of the few models of aSyn aggregation in cultured cells.

1. Introduction

Alpha Synuclein (aSyn) is an abundant, intrinsically disordered protein mainly localized in presynaptic terminals. aSyn folds into amphipathic alpha-helices in the presence of negatively charged lipids and can be divided into three distinct regions (Fig. 1A): the N-terminal region (residues 1–60), the central region (residues 61–95) originally known as non-amyloid component (NAC) region, and the C-terminal region (residues 96–140) [1,2]. The N-terminal region can adopt alpha-helical structure when associated with phospholipid membranes [3,4]. The central region is highly hydrophobic and essential for aggregation [5,6]. The C-terminal region is very acidic, is essential for the chaperone function of aSyn [7–9] and may modulate functions and interactions of the protein in the cellular environment [10].

Although the biological function of aSyn is still unclear, increasing evidence suggest it plays a major role in synaptic transmission and synaptic plasticity [11], where it regulates the vesicle release upon functional multimerization [12]. aSyn can misfold and accumulate in amyloid deposits known as Lewy bodies (LBs) that are typical pathological hallmarks in age-associated disorders named as

* Corresponding author at: Department of Experimental Neurodegeneration, University Medical Center Göttingen, Waldweg 33, 37073 Göttingen, Germany.
E-mail address: touteir@gwdg.de (T.F. Outeiro).
[1] Equal contribution.

https://doi.org/10.1016/j.bbapap.2019.140298
Received 4 July 2019; Received in revised form 7 October 2019; Accepted 8 October 2019
Available online 30 October 2019

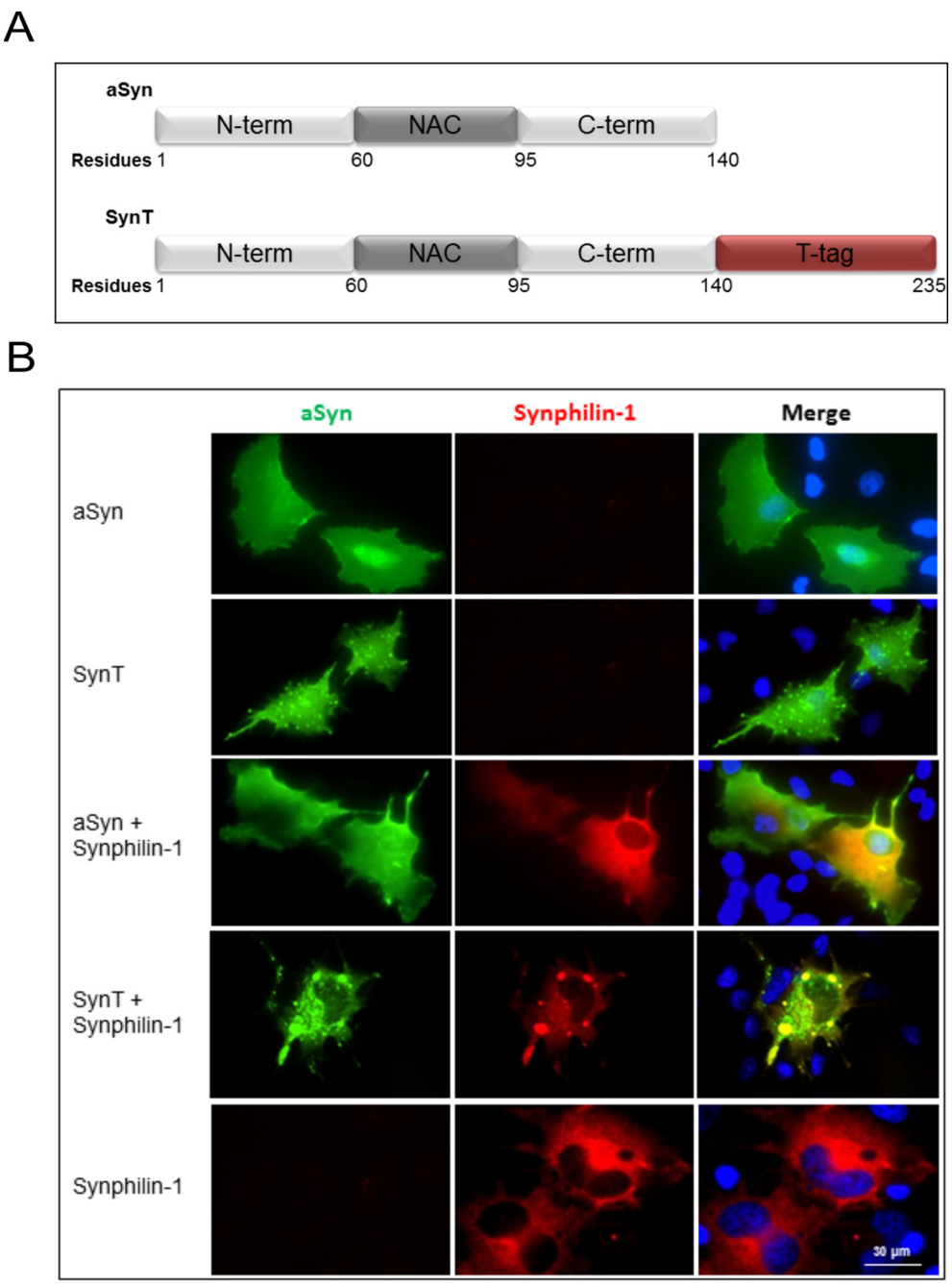

Fig. 1. C-terminal modified aSyn (SynT) forms inclusions in H4 cells. (A) Schematic representation of the structure of human aSyn highlighting the N-terminal (N-term), NAC (NAC) and C-terminal (C-term) regions of the protein. Amino acid residue numbers are indicated for aSyn and for SynT. (B) aSyn distribution in cells transfected with aSyn, SynT and SynT + Synphilin-1. In cells transfected with aSyn, or with aSyn + Synphilin-1, aSyn is diffusely distributed throughout the cell. In contrast, in cells transfected with SynT, or with SynT + Synphilin-1, aSyn forms inclusions of various sizes and morphologies. Cell nuclei were labeled with DAPI and are artificially colored in blue.

synucleinopathies. These include Parkinson's Disease (PD), multiple system atrophy, and Dementia with Lewy Bodies (DLB) [13–15].

aSyn aggregates are highly polymorphic, ranging from soluble oligomeric forms to ring- or string-like oligomers, spherical-shaped protofibrils, and insoluble fibrils [16–18]. The precise correlation between aSyn aggregation and neurotoxicity is unclear. aSyn fibrils seem to be critical for disease spreading and exogenously added fibrils can seed aSyn aggergation in cell models [19,20]. However, oligomeric forms of aSyn are hypothesized to be the most cytotoxic forms of the protein, rather than mature fibrillar aggregates [21–23]. To address this hypothesis, it is important to use cell and animal models that recapitulate central aspects of aSyn biology and aggregation. A commonly used cell-based model enables the visualization of aSyn oligomers in living cells *via* a bimolecular fluorescence complementation assay (BiFC) [24]. Currently, we lack models that mimic the process of formation of LB-like inclusions in cells just based on the expression of wild type (WT) aSyn. SynT, a modified form of aSyn displays a higher propensity to aggregate and leads to the formation of inclusions that resemble LBs upon co-expression with synphilin-1, a known aSyn-interacting protein that is also present in LBs [25,26]. SynT consists of a modified form of aSyn with a C-terminal extension, derived from the proteolytic cleavage of enhanced green fluorescent protein (EGFP) (amino acids 1–83, Fig. 1A), that makes aSyn more prone to aggregation. Thus, this powerful and versatile system has been extensively used to model aSyn aggregation in mammalian systems [27–33]. However, the C-terminal extension may alter the biochemical and biophysical properties of aSyn and, therefore, it is essential to characterize the molecular effects of this extraneous amino acid sequence in SynT in order to demonstrate the validity of the model. In this study, we used nuclear magnetic resonance (NMR) to investigate the structural and dynamic features of SynT and to demonstrate its usefulness and validity as a model of aSyn aggregation.

Interestingly, our results indicate that the conformations adopted by

aSyn in its SynT form resemble those of the unmodified protein. We detected differences in the N-terminal region, likely involving transient intra and/or intermolecular interactions. The steric hindrance at the C-terminus and the altered transient interactions at the N-terminal region of aSyn might be the factors behind the decreased membrane binding capacity of SynT compared to the unmodified protein species. Altogether, our work provides novel insights into the molecular determinants of aSyn aggregation and demonstrates the relevance of using SynT as a model for studying aSyn aggregation. Experimental strategies that enable the analysis of aSyn aggregation are critical for the identification of anti-aggregation strategies that can form the basis of future therapies for PD and other synucleinopathies.

2. Results

2.1. C-terminally-modified aSyn forms inclusions in cultured cells

As previously described, truncations and C-terminal modifications of aSyn alter its propensity to aggregate [26,34]. We have used human H4 neuroglioma cells, a widely used cell line to study cellular and molecular aspects of various neurodegenerative diseases, in order to investigate the effect of the C-terminal modification in aSyn (called SynT) cytoplasmic inclusions [35]. Expression of SynT resulted in the formation of cytosolic inclusions that exhibit LB-like properties [24,26] (Fig. 1B, Fig. S1). Inclusion formation is potentiated by the co-expression of SynT together with synphilin-1, an interactor of aSyn that is also present in LBs and Lewy neurites, as extensively described by several groups [24,30,36]. In contrast, co-expression of untagged aSyn with synphilin-1 did not result in the formation of discrete inclusions (Fig. 1B), suggesting that modifications in the C-terminal region altered the aggregation properties of aSyn.

2.2. Conformational and dynamic properties of the SynT variant

To analyze the impact that the C-terminal modification in SynT might have on the structural features of aSyn, we used NMR spectroscopy to assess the conformational and dynamic features of the ^{15}N isotopically labeled recombinant aSyn and SynT proteins. Given that the majority of aSyn in the cell is N-terminally acetylated, we used N-terminally acetylated aSyn and SynT throughout our study (Anderson 2006, Ohrfelt 2011).

Prior to the NMR measurements, we analyzed the recombinant N-terminally-acetylated SynT by SDS-PAGE and by gel-filtration chromatography to confirm the purity of the protein (Fig. S2 A-C). Then, NMR spectroscopy of backbone amides in ^{15}N-labeled SynT samples demonstrated that the SynT protein remains intrinsically disordered upon the C-terminal modification with the EGFP fragment. As expected, backbone chemical shift changes were observed in a discrete number of residues located in the vicinity of the EGFP fragment at the C-terminal region of the aSyn protein (Fig. 2A). Interestingly, small but measurable chemical shift changes became also evident in the region encompassing amino acids 1–10 (Fig. 2A), well distant from the C-terminus. Thus, the anchoring of the truncated EGFP segment at the C-terminus of aSyn in the SynT variant affects the chemical shift of resonances belonging to residues in both the C- and N-terminal region. Consistently, when the SynT/aSyn intensity ratio of backbone amide resonances was measured, a substantial reduction in the I/Io values was observed both at the N-terminus and the C-terminal residues that are proximal to the EGFP fragment (Fig. 2B). Interestingly, the degree of broadening of resonances in the most affected residues in the N-terminal region were almost similar to those observed at the C terminus. Finally, we observed that resonances located at the NAC region were also affected, although to a lesser extent.

These observations led us to evaluate the conformation of SynT and its dynamic properties. First, we measured a nearly complete set of $^{3}J_{HN\text{-}H\alpha}$ couplings in both aSyn and SynT states, which are particularly reliable quantitative reporters of the time-averaged distribution of the backbone torsion angles ϕ[39]. The values measured for the two forms of the protein are essentially indistinguishable, indicating that the C-terminal modification with the EGFP fragment in the SynT form did not influence substantially the local conformational propensities adopted by untagged aSyn (Fig. 3A).

Next, we evaluated the backbone dynamics of SynT. To this purpose, we measured ^{15}N R_1 and R_2 relaxation rates and heteronuclear (^{1}H − ^{15}N) nuclear Overhauser effects (hetNOEs). Whereas structures persisting on supra-τ_c (τ_c = overall tumbling time) can be monitored by chemical shifts and scalar coupling constants (J), ^{15}N relaxation rates and hetNOEs are sensitive to motions faster than the overall tumbling time in the sub-nanosecond time regime. The set of ^{15}N relaxation experiments was firstly measured on aSyn, in which the relaxation parameters showed a similar sequence dependence, with lower values at the termini of the protein and a plateau at the center of the relaxation profile. In agreement with previous results [40], R_1 values ranged between 1.3 and 1.7 s-1, R_2 values between 2.0 and 3.5 s-1, and hetNOEs values were found in the range 0 to −0.3 (Fig. 3B–D). The attachment of the EGFP fragment to aSyn resulted in no significant changes in the R_1 and hetNOEs values, with the exception of the very terminal residues. However, pronounced deviations were observed for the R_2 relaxation rates (Fig. 3C). Consistent with the broadening profile shown in Fig. 2B, R_2 rates were increased for the N-terminal half of the aSyn sequence when the EGFP fragment was attached at the C-terminus, which also experienced increased transverse relaxation. Whereas increased R_2 rates at the C-terminus can be connected to slower rotational tumbling of the beta-structure containing EGFP fragment (Fig. 2B), the faster transverse relaxation in the N-terminal half of the aSyn sequence points to an exchange process likely driven by transient interactions between the N-terminal region of aSyn and the EGFP fragment. Notably, higher R_2 rates were centered at the Y39 residue, suggesting contributions of aromatic interactions to the exchange process.

Overall, the results reported here allow us to conclude that the intrinsically disordered nature of aSyn is not strongly influenced by the C-terminal modification in SynT, whereas the transient long-range contacts between the N- and C-terminal regions reported for aSyn are strengthened in the SynT variant.

2.3. Molecular interactions driven by the N-terminal region are affected in the SynT variant

Since the N-terminal region of aSyn behaves as a key interface for physiological or pathological processes such as membrane binding or protein aggregation, we further investigated the influence of the EGFP fragment on the N-terminal region of aSyn through the analysis of its binding properties to lipids and small molecules with anti-amyloid activity.

First, we analyzed the binding features of SynT to small unilamellar vesicles (SUVs) with appropriate mixtures of DOPE, DOPC and DOPS that have been shown to model the biochemical composition of synaptic vesicles [38]. Although the slow tumbling rate of vesicles induces lipid-bound aSyn to exhibit dynamic properties that hamper its direct observation by solution NMR, exchange with the NMR-visible, lipid-free form allows residue-specific access to the properties of the membrane-bound state. We probed this exchange process using two-dimensional ^{1}H−^{15}N heteronuclear single quantum coherence (HSQC) experiments of 100 μM aSyn in the presence of SUVs (1:100 protein-to-lipid ratio). In line with previous studies, the NMR signal intensities of the 100 N-terminal residues of aSyn were strongly decreased compared with free aSyn (Fig. 4A). On the other hand, a smaller broadening effect was observed for the N-terminal region of the SynT species in its membrane-bound state, whereas its C-terminal region was more strongly affected by lipid-binding when compared to aSyn. These results suggest that a different anchoring mechanism may exist for aSyn and SynT binding to lipids.

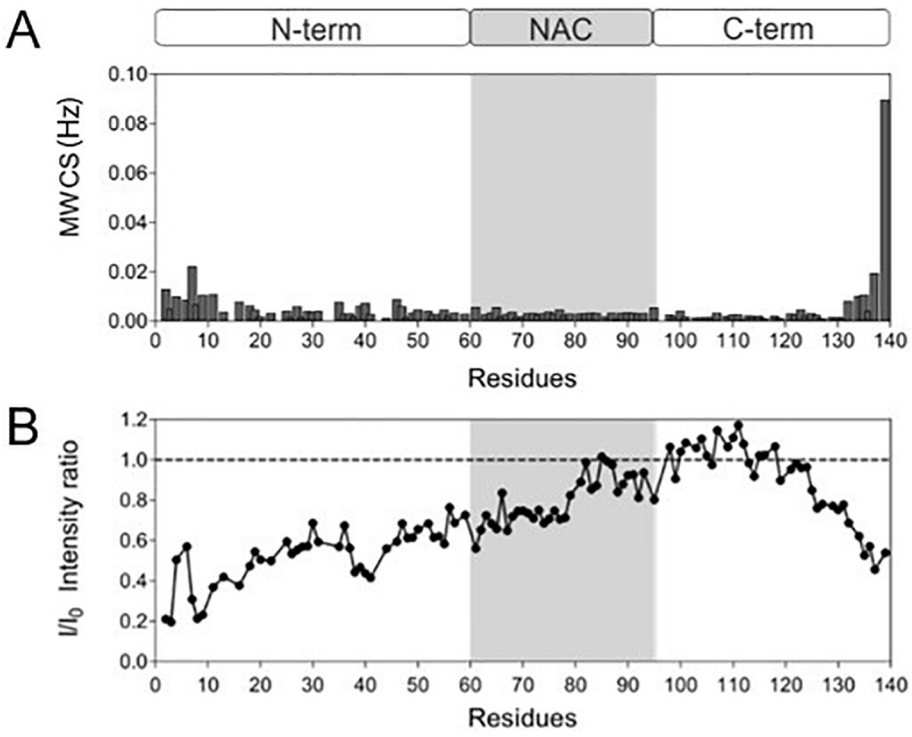

Fig. 2. NMR characterization of SynT. (A) Mean weighted $^{1}H-^{15}N$ chemical shift perturbation plot of Ac-SynT *versus* Ac-aSyn. (B) Ac-SynT/Ac-aSyn NMR signal intensity ratios. All NMR experiments were recorded at 15 °C using 100 μM aSyn and SynT samples dissolved in buffer B supplemented with 10% D_2O.

Finally, we used small molecules that bind exclusively to the N-terminal region of aSyn as molecular probes to monitor the impact of the EGFP fragment on the binding properties of the N-terminal interface. To this purpose, we used the molecule phthalocyanine tetrasulfonate (PcTS). The exclusive binding of this molecule to the N-terminal region of aSyn is regulated by the specific interaction of its macrocycle ring with aromatic residues located at that region (F4 and Y39), and by the electrostatic repulsions between the peripheral sulfonate groups in PcTS and the highly negatively charged C-terminal region that is folded back toward the NAC domain in the monomeric state of aSyn. As previously reported, PcTS binds preferentially to the N-terminal region of aSyn (Fig. 4B). In contrast, this interaction is abolished in the SynT variant, likely reflecting a change in the binding behavior of the N-terminal region toward PCTs molecules. However, the occurrence of a potential EGFP-PcTS interaction that sequesters small molecules from its binding to the N-terminus of SynT cannot be discarded at this point, and would have to be investigated in other studies.

2.4. SynT does not form amyloid fibrils in vitro

Next, we investigated whether the EGFP fragment affected the fibrilization of aSyn *in vitro*, since it affects the aggregation of the protein in cultured cells. Recombinant aSyn or SynT were incubated at 37 °C, under constant agitation, and fibrillization kinetics were monitored by Thioflavin T (ThT) binding. Surprisingly, SynT did not show any fibril-specific increase in ThT intensity *in vitro* (Fig. 4C).

Amyloid fibril formation was further assessed by transmission electron microscopy (TEM) analysis on negatively stained samples of aSyn and of SynT, after the aggregation protocol. Consistently with the ThT assay, we found that aSyn formed well-defined amyloid filaments (Fig. 4D). In contrast, SynT formed non-fibrillar aggregates.

3. Discussion

aSyn is the major component of pathognomonic protein inclusions in PD and other synucleinopathies, but the precise mechanisms underlying aggregation and pathology are still elusive [39]. aSyn is a paradigmatic example of an intrinsically disordered protein that is capable of adopting a multitude of conformations, depending on the environment where it occurs. For example, aSyn can exist as a soluble cytosolic protein, membrane-bound, or aggregated [40–42]. In order to understand the molecular determinants of aSyn aggregation, several *in vitro* and *in vivo* models have been employed, in an attempt to mimic the behavior of the protein in synucleinopathies. However, while aSyn is known to readily fibrilize in the test tube, it has not been possible to consistently induce aSyn aggregation in cultured cells, just based upon expression. To promote aSyn aggregation in cells, different strategies have been employed, including co-expression with other proteins [43], oxidative stress [44], metal ions [45,46], or the addition of extraneous amino acid sequences [26,47]. An alternative strategy involves the expression of an aSyn variant fused to a fragment of EGFP, thereby changing the chemical properties of the C-terminal region of aSyn. However, whether these manipulations mimic relevant aspects of aSyn pathobiology, or simply represent artificial phenotypes that are not accessible to the constellation of conformations aSyn can adopt remains unclear. In the present study, we compared SynT with normal untagged aSyn in terms of its folding and conformation. Our study clarifies the aggregation behavior of SynT in cells and demonstrates that SynT is a valid model of aSyn aggregation.

From a biophysical perspective, the NMR spectra and general dynamics of the protein backbone observed for aSyn and SynT demonstrate that the aSyn part of SynT retains the intrinsically disordered character of the untagged protein. However, we observed subtle changes in the conformational propensities of the protein ensembles. As expected, the C-terminal region of aSyn showed changes in the position and intensities of the NMR signals, likely due to changes in the chemical environment induced by the nearby EGFP fragment and its contribution to the local rotational correlation time. On the other hand, we also detected an attenuation of the intensity of the signal of the amide signals in the N-terminal region of SynT that correlated well with a chemical exchange process detected by 15 N spin relaxation measurements. Taken together, these results suggest that the EGFP fragment might transiently interact with the N-terminus of the protein in an inter- or intra-molecular manner (Fig. 5). Intramolecular contacts between the C– and N-Terminus have been described and were proposed to regulate

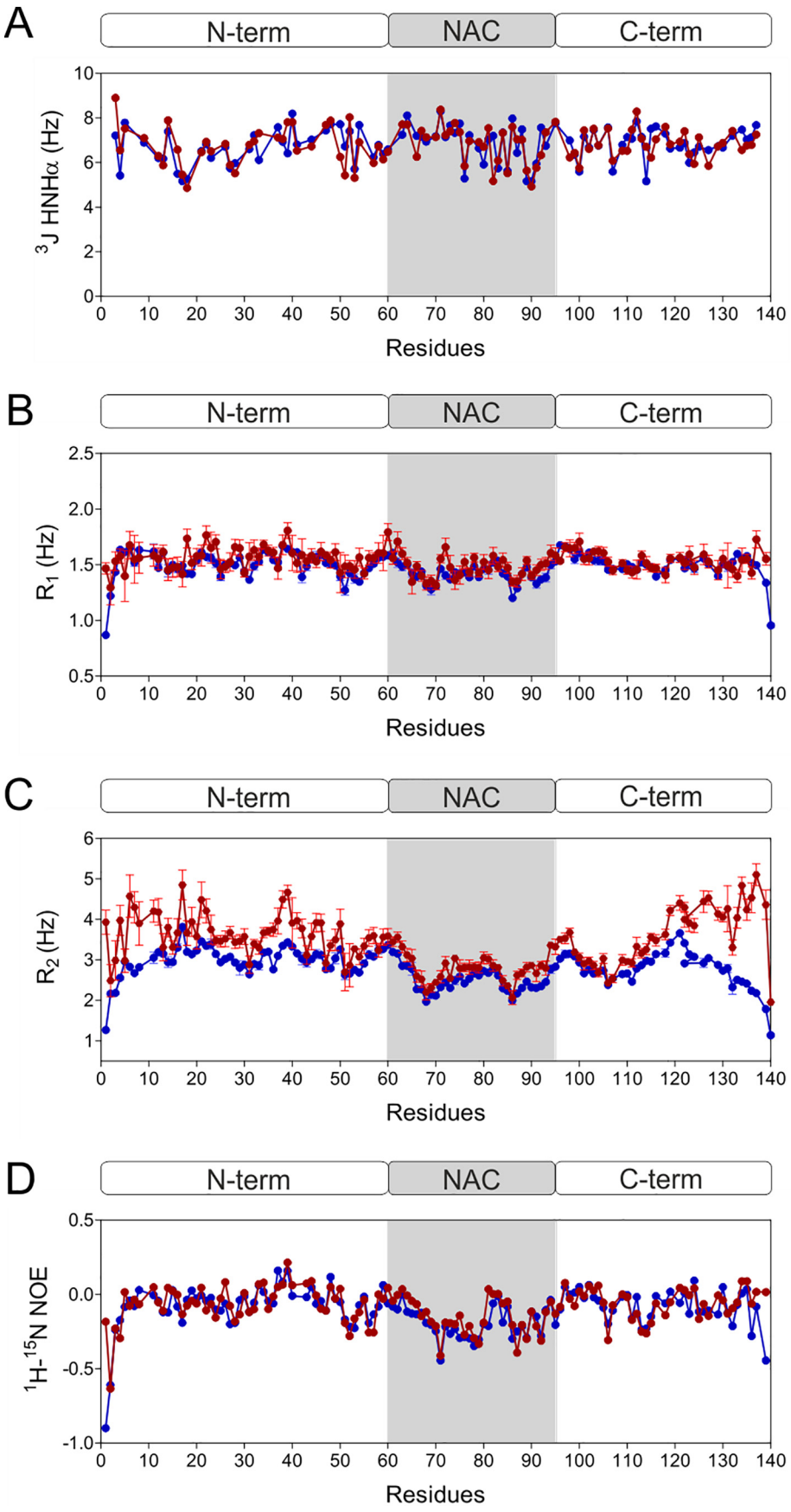

Fig. 3. Backbone dynamics of SynT. (A) ^{3}J HN-Hα coupling constants measured for Ac-aSyn (blue) and Ac-SynT (red). (B,C) ^{15}N relaxation rates of Ac-aSyn (blue) and Ac-SynT (red). Panels (B) and (C) depict R_1 and R_2 rates, respectively. Panel (D) shows ^{1}H−^{15}N hNOE profiles for both proteins. All experiments were recorded at 15 °C using Ac-aSyn (100 μM) and Ac-SynT (100 μM) dissolved in buffer B supplemented with 10% D_2O.

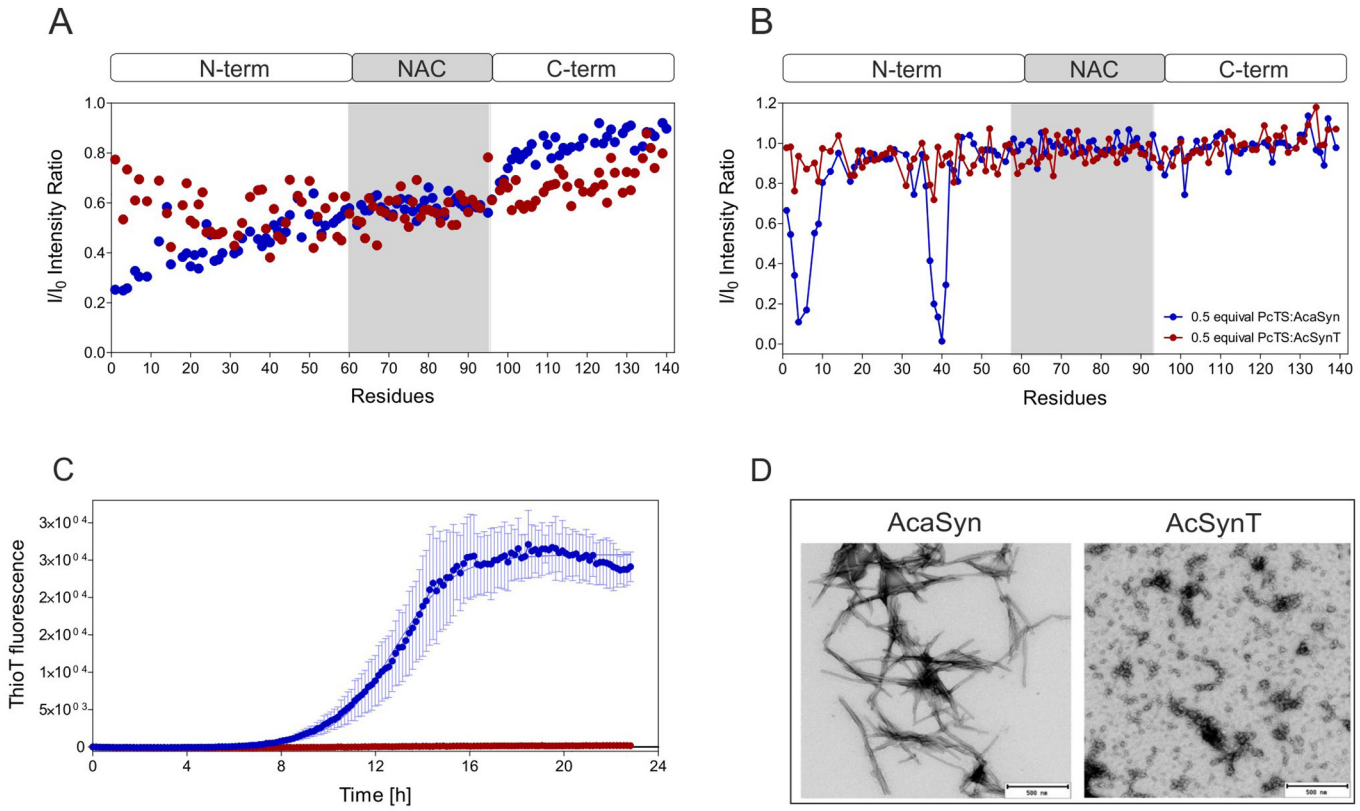

Fig. 4. Binding and aggregation properties of Ac-SynT.
Membrane binding properties of Ac-aSyn (Blue) and Ac-SynT (red) in the presence of artificial small unilamellar vesicles membranes (SUVs) [1:100 protein:SUVs ratio] (A). Interaction profiles of the backbone amide groups of 10 μM Ac-aSyn, in blue and 90 μM Ac-SynT proteins, in red, in the presence of 50 μM of PcTS (B). Continuous ThioT aggregation assays of a 25 μM solutions of Ac-aSyn (blue) and Ac-SynT (red). The proteins were diluted in Buffer A (25 mM Tris, pH 7.7) (C). TEM images of the resulting aggregates stained with uranyl acetate (scale bar, 500 nm) (D).

the major events of nucleation [40,48,49]. These long-range contacts determine the "open" conformation of the molecule that allows aggregation and alterations of these long-range contacts promotes exposure of the fibrillating segment of the NAC region, hence enhancing the aggregation propensity [49,50].

This transient interaction could explain the attenuated ability of the N-terminal residues of SynT to interact with the small molecule PcTS and could contribute to the altered binding mode of SynT with membranes. Interestingly, it was previously shown that transient interactions between C- and N-Terminus result in the formation of compact aggregation-resistant structures [51]. We hypothesize that the proximity of the tag could create steric disturbances that influence how SynT interacts with membranes and folds into alpha-helical structures on the membrane surface. Considering recent findings that indicate aSyn aggregation is increased when aSyn is in its unstructured monomeric form, and is attenuated/blocked when it is in an alpha-helical multimeric form associated with membranes [52], our results suggest that the perturbed interaction of SynT with membranes might, at least

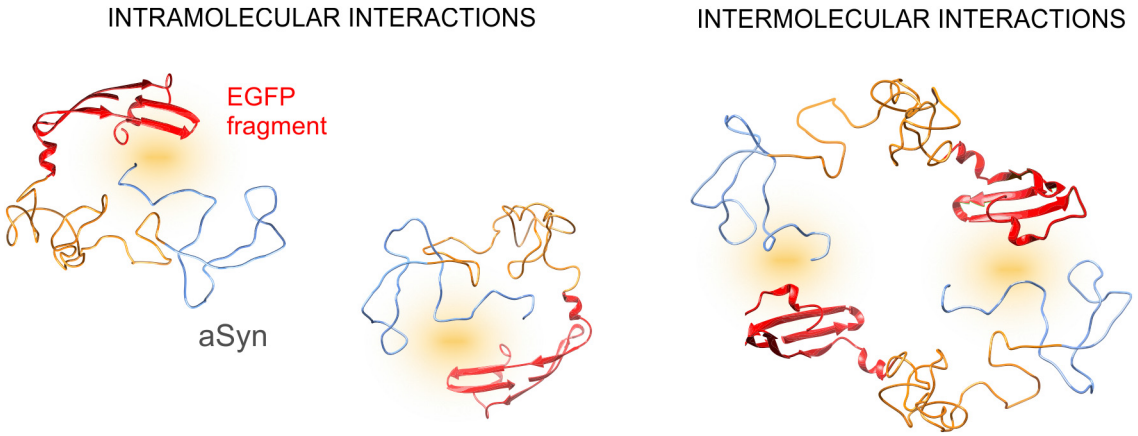

Fig. 5. Proposed mechanism for the structural properties of SynT. The EGFP fragment could transiently interact with the N-terminal region of the protein in an intermolecular or in an intra-molecular way. Overall, the general, chemical properties of aSyn are not affected by the tag, nor its propensity to maintain an intrinsically disordered structure. Still, some of the physiological-related properties of aSyn appear to be affected by the tag (e.g., membrane binding properties and aggregation propensities *in vivo* and *in vitro*).

in part, be responsible for its increased aggregation propensity in cells. Several studies have investigated the relationship between membrane interactions and aSyn aggregation but, nevertheless, the mechanisms by which lipids or lipid vesicles influence the aggregation of aSyn are still not fully understood [53–56].

It has also been shown that the acidic C-terminal region of aSyn can play a role and affect the aggregation properties of aSyn both in monomeric and aggregated forms [10]. The aggregation kinetics are sensitive to a wide range of ionic conditions [57], from weak C-terminal charge shielding [10] to stronger charge modifications caused by the presence of polycations [58] or metal ions [45,46,59,60], PTMs [60,61], truncations [62,63] or, as in the case of our study, the addition of tags [26]. Thus, it is possible that, due to the presence of the tag, changes in the electrostatic environment of this region of the protein may overall affect the aggregation behaviour.

Taken together our study indicates that the modification of the C-terminus of aSyn in SynT, and the subsequent effect on the N-terminal region, potentiates the ability of the protein to form intracellular inclusions, which recapitulates important molecular features of synucleinopathies. Cellular models based on expression of aSyn variants such as SynT are widely used tools for the identification of genetic and pharmacological strategies to treat PD and other synucleinopathies. Given the similarities observed between SynT and aSyn in terms of folding and conformation, our study demonstrates the usefulness of SynT as a model for aSyn aggregation.A detailed understanding of the molecular mechanisms underlying aSyn aggregation, as afforded by the SynT model, is important for the development of novel therapeutic strategies for these devastating disorders.

4. Materials and methods

4.1. Human cell cultures

Human neuroglioma H4 cells were maintained at 37 °C and 5% CO_2 environment, in Opti-Mem medium (PAN, Germany) supplemented with 10% foetal calf serum (ThermoFisher) and 1% penicillin-streptomycin (ThermoFisher). Cells were seeded in different well-plate formats, one day prior to transfection, and kept up to 48 h after transfection. Transfections were performed with calcium phosphate. Shortly, 3 h prior to transfection, fresh medium was added to the cells. DNA was diluted in 1× HBS buffer with 25 mM 4-(2-hydroxyethyl)-1-piperazineethanesulfonic acid, 140 mM NaCl, 5 mM KCl, 0.75 mM $Na_2HPO_4 \cdot 2H_2O$, 6 mM Dextrose, pH 7.1. After mixing, 2.5 M $CaCl_2$ was added dropwise and vigorously mixed. Followed 20 min of incubation, the mixture was added dropwise to the cells. Medium was replaced the next morning. For total protein extraction, cells were lysed 48 h after transfection in Radio-Immunoprecipitation Assay (RIPA) lysis buffer (50 mM Tris pH 8.0, 0.15 M NaCl, 0.1% SDS, 1% NP40, 0.5% Na-Deoxycholate, 2 mM EDTA and a Protease Inhibitor Cocktail (1 tablet/10 mL) (Roche Diagnostics, Mannheim, Germany)). The protein concentration was measured using a Bradford assay (BioRad Laboratories, Hercules, CA, USA).

4.2. Immunocytochemistry

24 or 48 h after transfection, H4 cells were washed with PBS and fixed with 4% paraformaldehyde (PFA) for 10 min at room temperature (RT), followed by a permeabilization step with 0.5% Triton X-100 (SigmaAldrich, St. Louis, MO, USA) for 10 min at RT. After blocking in 10% normal goat serum (PAA, Cölbe, Germany)/DPBS for 1 h, cells were incubated with primary antibody. Primary antibodies used were: rabbit anti-aSyn (aSyn Antibody (C-20): sc-7011-R, 1:1000, Santa Cruz Biotechnology, Dallas, USA) or mouse anti-V5 (v5 Mouse monoclonal Antibody, R960–25, 1:1000, Invitrogen, Thermofisher), for 3 h or overnight and secondary antibody (Alexa Fluor 488 donkey anti-mouse IgG and/or Alexa Fluor 555 goat anti rabbit IgG, (Life Technologies-Invitrogen, Carlsbad, CA, USA) for 2 h at RT. Finally, cells were stained with Hoechst 33258 (Life Technologies- Invitrogen, Carlsbad, CA, USA) (1:5000 in DPBS) for 5 min, washed again and then fixed with Mowiol for epifluorescence microscopy.

4.3. Protein purification

^{15}N isotopically enriched and N-terminally acetylated aSyn and SynT were obtained by transfecting *E. coli* BL21 competent cells with a pET21 carrying the wild type aSyn gene or the SynT gene together with a second plasmid encoding the components of yeast NatB acetylase complex [64]. Plasmids carried different antibiotic resistance (ampicillin and chloramphenicol) to select the doubly transformed *E. coli* colonies. Both proteins were purified as previously reported [10]. Protein concentration was estimated from the absorbance at 274 nm using an extinction coefficient of 5600 $M^{-1}\,cm^{-1}$ for aSyn, and of 16,055 $M^{-1}\,cm^{-1}$ for SynT. Protein acetylation was verified *via* mass spectrometry.

4.4. Immunoblotting

40 µg of total protein from cell extracts was boiled for 10 min at 100 °C in sample buffer (125 mM of 1 M Tris HCl pH 6.8, 4% SDS 0,5% Bromphenol blue, 4 mM EDTA 20% Glycerol 10% β-Mercaptoethanol) and subsequently separated by SDS-Page in a 15% polyacrylamide separation gel and a 6% polyacrylamide stacking gel (Bio-Rad, Hercules, CA, USA). Proteins were transferred to a nitrocellulose membrane using a Mini Trans-Blot system (BioRad Laboratories, Hercules, CA, USA). Western Blotting was performed using standard procedures. The following antibodies were used: anti-V5 (for detection of synphilin-1, 1:1000, Abcam, Boston, USA), anti-Syn1 (1:1000, BD Biosciences, San Jose, CA, USA), anti a-Tubulin-1 (1:2000, SigmaAldrich, St. Louis, MO, USA).

4.5. NMR experiments

All NMR spectra were recorded on Bruker 600 MHz Avance III spectrometer, equipped with a cryogenically cooled triple resonance ^1H ($^{13}C/^{15}N$) TCI probe. $^1H-^{15}N$ SOFAST-HMQC [65], $^1H-^{15}N$ HSQC, ^{15}N R_1 and ^{15}N R_2 relaxation rates, $^1H-^{15}N$ heteronuclear NOE and 3D HNHA experiments were recorded at 15 °C using protein samples dissolved in buffer B (20 mM MES, NaCl 100 mM, pH 6.5) supplemented with 10% D_2O.

$^1H-^{15}N$ SOFAST-HMQC and $^1H-^{15}N$ HSQC: we used 16 scans, 1024 complex points (sweep-width of 16 ppm in the ^1H dimension) and 256 complex points (sweep-width of 26 ppm in the ^{15}N dimension). Sequence-specific assignments for the backbone of aSyn and SynT were transferred from previously published work [59,66]. Only unambiguously assigned, well resolved peaks were included in the analysis. The I/I_0 ratios obtained for aSyn and SynT, in absence and presence of PcTS or SUVs were plotted as a function of the protein sequence to obtain the intensity perturbation profiles [67]. Mean weighted chemical shifts displacements (MWΔCS) for $^1H-^{15}N$ were calculated as as $[(\Delta\delta^1H)^2 + (\Delta\delta^{15}N/10)^2]^{1/2}$.

^{15}N R_1 and R_2 relaxation rates, and $^1H-^{15}N$ NOE data were acquired at 600 MHz external field using previously described pulse sequences [68]. Experiments were recorded with 1024 complex points and a sweep width of 16 ppm for the ^1H dimension, and 256 complex points in the ^{15}N dimension with a sweep width of 26 ppm. R_1 and R_2 relaxation rates were obtained by recording the experiments with different T_1 and T_2 relaxation delays. Resonance heights in the spectra at each delay were fit to a two parameter exponential decay function to obtain the rates. Steady-state $^1H-^{15}N$ NOE (hetNOEs) values were obtained from the ratio of peak heights in spectra collected with and without an initial 4 s period of proton saturation during the recycling delay.

HN-Hα experiments were recorded with the following set up: number of points, 1024 (^{1}H), 80 (^{15}N), 144 (^{1}H); spectral width (ppm), 16 (^{1}H), 26 (^{15}N), 10 (1H); number of scans, 16. Three-bond HN-Hα coupling constants (^{3}J HN-Hα) were obtained from the ratio between the intensities of the diagonal peaks and cross-peaks in the HN-Hα correlation region [69]. Three-bond HN-Hα coupling constants (^{3}J HN-Hα) are sensitive to the torsion angle ϕ populated by each amide group in the protein backbone reporting on secondary structure content. This coupling falls in the range 3.0–6.0 Hz for an α-helix and 8.0–11.0 Hz for a β-sheet structure. For a random-coil, a weighted average of these values is observed, that typically ranges between 6.0 and 8.0 Hz for most residues [70].

Acquisition and processing of NMR spectra were performed using TOPSPIN 3.2 (Bruker Biospin). 2D spectra analyses were performed with CCPN. For the ^{3}J HN-Hα couplings calculation, the software CARA was used. R_1 and R_2 relaxation data fitting was performed using CCPN routines.

4.6. SUVs preparation

SUVs were prepared from a molar ratio of 1:1 of Coagulation Reagent I containing DOPE:DOPS:DOPC (5:3:2 w/w) and DOPC (both Avanti Polar Lipids Inc., USA) dissolved in chloroform yielding a final molar ratio of DOPE:DOPS:DOPC (5:3:12 w/w). The lipid solution formed a thin film under evaporation of the solvent with nitrogen gas and was further dried by lyophilization under vacuum. The dried phospholipids were dissolved in MES buffer (20 mM MES, 100 mM NaCl, pH 6.5) and underwent several cycles of freeze-thawing and water bath sonication until the solution became clear. The size distribution was also checked by DLS. For the NMR experiments a SUV stock solution of 85 mM (6.6% w/v) in respect to the monomers was used.

4.7. Thioflavin T fluorescence assays

In vitro aggregation kinetics was obtained using a PolarStar OMEGA microplate reader. The plate was shaken at 300 rpm/37 °C and fibril formation was monitored by measuring Thioflavin-T (ThT) fluorescence every 5 min. The excitation wavelength was set to 440 nm and the Thio-T emission was measured at 480 nm. Each well contained 150 μL of 25 μM AcaSyn or 25 μM AcSynT (Buffer A), 1 μM Thio-T, and a 2 mm glass bead to accelerate fibrillation. In all cases, the reported values correspond to the average of five independent aggregation measurements.

4.8. Transmission electron Microscopy

Samples were shaken at 300 rpm/37 °C for 3 days, adsorbed onto carbon-coated grids, rinsed with water, and stained with 2% (wt/vol) uranyl acetate. The samples were exhaustively scanned and representative fields were imaged in a Hitachi H-7000 TEM operating at an accelerating voltage of 75 kV.

Declaration of Competing Interest

The authors declare that they have no conflicts of interest with the contents of this article.

Acknowledgements

TFO and MZ are supported by the DFG Center for Nanoscale Microscopy and Molecular Physiology of the Brain (CNMPB), and TFO by the State of Lower Saxony, Hannover, Germany MWK). COF thanks ANPCyT, FONCyT, Fundacion Medife, Fundacion Bunge y Born, Max Planck Society and Alexander von Humboldt Foundation for financial support. CM thanks Maria E. Chesta and Marco C. Miotto for helpful discussions. CM and TS received PhD Fellowships from the CUAA-DAHZ Deutsch-Argentinisches Hochschulzentrum.

Appendix A. Supplementary data

Supplementary data to this article can be found online at https://doi.org/10.1016/j.bbapap.2019.140298.

References

[1] Maroteaux, Luc, J.T. C, R.H. S, Synuclein : a neuron-specific protein localized to the nucleus and presynaptic nerve terminal, J. Neurosci. 8 (1988) 2804–2815.
[2] R.J. Perrin, W.S. Woods, D.F. Clayton, J.M. George, Interaction of human a-Synuclein and Parkinson ' s disease variants with phospholipids, J. Biol. Chem. 275 (2000) 34393–34398.
[3] S. Chandra, X. Chen, J. Rizo, R. Jahn, T.C. Su, A broken a-helix in folded a-Synuclein, J. Biol. Chem. 278 (2003) 15313–15318.
[4] R.J. Bussell, D. Eliezer, A structural and functional role for 11-mer repeats in a -Synuclein and other exchangeable lipid binding proteins, J. Mol. Biol. 2836 (2003) 763–778.
[5] B.I. Giasson, I.V.J. Murray, J.Q. Trojanowski, V.M. Lee, A hydrophobic stretch of 12 amino acid residues in the middle of a-Synuclein is essential for filament assembly, J. Biol. Chem. 276 (2001) 2380–2386.
[6] H. Du, L. Tang, X. Luo, H. Li, J. Hu, J. Zhou, H. Hu, A peptide motif consisting of glycine, alanine, and valine is required for the fibrillization and cytotoxicity of human a-synuclein, Biochemistry 42 (29) (2003 Jul 29) 8870–8878.
[7] M.Y. Souza, B.I. Giasson, V.M. Lee, H.I. Y, Chaperone-like activity of synucleins, FEBS Lett. 474 (2000) 116–119.
[8] S.M. Park, H.Y. Jung, T.D. Kim, J.H. Park, C. Yang, J. Kim, Distinct roles of the N-terminal-binding domain and the C-terminal-solubilizing domain of A-Synuclein, a molecular chaperone, J. Biol. Chem. 277 (2002) 28512–28520.
[9] T.D. Kim, S.R. Paik, C.-H. Yang, Structural and functional implications of C-terminal regions of alpha-synuclein, Biochemistry 41 (2002) 13782–13790.
[10] W. Hoyer, D. Cherny, V. Subramaniam, T.M. Jovin, Impact of the acidic C-terminal region comprising amino acids 109 - 140 on a-Synuclein aggregation in vitro, Biochemistry 43 (51) (2004 Dec 28) 16233–16242.
[11] S. Liu, I. Ninan, I. Antonova, F. Battaglia, F. Trinchese, A. Narasanna, N. Kolodilov, W. Dauer, D. Hawkins, O. Arancio, A -Synuclein produces a long-lasting increase in neurotransmitter release, EMBO J. 23 (2004) 4506–4516.
[12] J. Burré, M. Sharma, T.C. Südhof, A-Synuclein assembles into higher-order multimers upon membrane binding to promote SNARE complex formation, Proc. Natl. Acad. Sci. (2014), https://doi.org/10.1073/pnas.1416598111.
[13] M.G. Spillantini, M.L. Schmidt, V.M.-Y. Lee, J.Q. Trojanowski, M. Goedert, A-Synuclein in Lewy bodies, Nature 388 (6645) (1997 Aug 28) 839–840.
[14] S. Arawaka, Y. Saito, S. Murayama, H. Mori, Lewy body in neurodegeneration with brain iron accumulation type 1 is immunoreactive for a-ynuclein, Am. Acad. Neurol. 51 (3) (1998 Sep) 887–889.
[15] K. Wakabayashi, M. Yoshimoto, S. Tsuji, H. Takahashi, A -Synuclein immunoreactivity in glial cytoplasmic inclusions in multiple system atrophy, Neurosci. Lett. 249 (1998) 180–182.
[16] J. Rochet, K.A. Conway, P.T. Lansbury, Inhibition of fibrillization and accumulation of prefibrillar oligomers in mixtures of human and mouse a-Synuclein, Biochemistry 39 (35) (2000 Sep 5) 10619–10626.
[17] T.T. Ding, S. Lee, J. Rochet, P.T. Lansbury, Annular a-Synuclein Protofibrils are produced when spherical Protofibrils are incubated in solution or bound to brain-derived membranes †, Biochemistry 41 (32) (2002 Aug 13) 10209–10217.
[18] H.A. Lashuel, B.M. Petre, J. Wall, M. Simon, R.J. Nowak, T. Walz, P.T.L. Jr, A -synuclein, especially the parkinson ' s Disease- associated mutants, forms pore-like annular and tubular protofibrils, J. Mol. Biol. 2836 (2002) 1089–1102.
[19] K.C. Luk, C. Song, P. O'Brien, A. Stieber, J.R. Branch, K.R. Brunden, J.Q. Trojanowski, V.M.-Y. Lee, Exogenous alpha-synuclein fibrils seed the formation of Lewy body-like intracellular inclusions in cultured cells, Proc. Natl. Acad. Sci. U. S. A. 106 (2009) 20051–20056.
[20] L.A. Volpicelli-Daley, K.C. Luk, V.M.-Y. Lee, Addition of exogenous α-synuclein preformed fibrils to primary neuronal cultures to seed recruitment of endogenous α-synuclein to Lewy body and Lewy neurite-like aggregates, Nat. Protoc. 9 (2014) 2135–2146.
[21] D.P. Karpinar, M. Babu, G. Balija, S. Ku, F. Opazo, N. Rezaei-ghaleh, N. Wender, H. Kim, H. Heise, A. Kumar, L. Fichtner, A. Voigt, G.H. Braus, K. Giller, A. Herzig, M. Baldus, S. Eimer, B. Schulz, C. Griesinger, M. Zweckstetter, Pre-fibrillar a -synuclein variants with impaired b -structure increase neurotoxicity in Parkinson ' s disease models, EMBO J. 28 (2009) 3256–3268.
[22] L. Breydo, J.W. Wu, V.N. Uversky, Biochimica et Biophysica Acta α -Synuclein misfolding and Parkinson ' s disease, BBA Mol. Basis Dis. 1822 (2012) 261–285.
[23] H.A. Lashuel, C.R. Overk, A. Oueslati, E. Masliah, The many faces of α-synuclein: from structure and toxicity to therapeutic target, Nat. Rev. Neurosci. 14 (2013) 38–48.
[24] D.F. Lázaro, E.F. Rodrigues, R. Langohr, H. Shahpasandzadeh, T. Ribeiro, P. Guerreiro, E. Gerhardt, K. Kröhnert, J. Klucken, M.D. Pereira, B. Popova, N. Kruse, B. Mollenhauer, S.O. Rizzoli, G.H. Braus, K.M. Danzer, T.F. Outeiro, Systematic comparison of the effects of alpha-synuclein mutations on its oligomerization and aggregation, PLoS Genet. 10 (2014) e1004741.
[25] P. Wales, D.F. Lázaro, R. Pinho, T.F. Outeiro, Limelight on alpha-synuclein:

pathological and mechanistic implications in neurodegeneration, J. Park. Dis. 3 (2013) 415–459.
[26] P.J. McLean, H. Kawamata, B.T. Hyman, α-Synuclein-enhanced green fluorescent protein fusion proteins form proteasome sensitive inclusions in primary neurons, Neuroscience 104 (2001) 901–912.
[27] H. Vicente Miranda, É. Szegő, L.M.A. Oliveira, C. Breda, E. Darendelioglu, R.M. de Oliveira, D.G. Ferreira, M.A. Gomes, R. Rott, M. Oliveira, F. Munari, F.J. Enguita, T. Simões, E.F. Rodrigues, M. Heinrich, I.C. Martins, I. Zamolo, O. Riess, C. Cordeiro, A. Ponces-Freire, H.A. Lashuel, N.C. Santos, L.V. Lopes, W. Xiang, T.M. Jovin, D. Penque, S. Engelender, M. Zweckstetter, J. Klucken, F. Giorgini, A. Quintas, T.F. Outeiro, Glycation potentiates α-synuclein-associated neurodegeneration in synucleinopathies, Brain 140 (2017) 1399–1419.
[28] R.M. de Oliveira, H. Vicente Miranda, L. Francelle, R. Pinho, É. Szegö, R. Martinho, F. Munari, D.F. Lázaro, S. Moniot, P. Guerreiro, L. Fonseca, Z. Marijanovic, P. Antas, E. Gerhardt, F.J. Enguita, B. Fauvet, D. Penque, T.F. Pais, Q. Tong, S. Becker, S. Kügler, H.A. Lashuel, C. Steegborn, M. Zweckstetter, T.F. Outeiro, The mechanism of sirtuin 2–mediated exacerbation of alpha-synuclein toxicity in models of Parkinson disease, PLoS Biol. 15 (2017) e2000374.
[29] A. Kleinknecht, B. Popova, D.F. Lázaro, R. Pinho, O. Valerius, T.F. Outeiro, G.H. Braus, C-terminal tyrosine residue modifications modulate the protective phosphorylation of serine 129 of α-Synuclein in a yeast model of Parkinson's disease, PLoS Genet. 12 (2016) e1006098.
[30] J. Klucken, A.-M. Poehler, D. Ebrahimi-Fakhari, J. Schneider, S. Nuber, E. Rockenstein, U. Schlötzer-Schrehardt, B.T. Hyman, P.J. McLean, E. Masliah, J. Winkler, Alpha-synuclein aggregation involves a bafilomycin A $_1$ -sensitive autophagy pathway, Autophagy 8 (2012) 754–766.
[31] T. Lopes da Fonseca, R. Pinho, T.F. Outeiro, A familial ATP13A2 mutation enhances alpha-synuclein aggregation and promotes cell death, Hum. Mol. Genet. 25 (2016) ddw147.
[32] A.J. Harrington, T.A. Yacoubian, S.R. Slone, K.A. Caldwell, G.A. Caldwell, Functional analysis of VPS41-mediated Neuroprotection in *Caenorhabditis elegans* and mammalian models of Parkinson's disease, J. Neurosci. 32 (2012) 2142–2153.
[33] D. Macedo, C. Jardim, I. Figueira, A.F. Almeida, G.J. McDougall, D. Stewart, J.E. Yuste, F.A. Tomás-Barberán, S. Tenreiro, T.F. Outeiro, C.N. Santos, (Poly) phenol-digested metabolites modulate alpha-synuclein toxicity by regulating proteostasis, Sci. Rep. 8 (2018) 6965.
[34] A.W. Michell, G.K. Tofaris, H. Gossage, P. Tyers, M.G. Spillantini, R.A. Barker, The effect of truncated human alpha-synuclein (1−120) on dopaminergic cells in a transgenic mouse model of Parkinson's disease, Cell Transplant. 16 (2007) 461–474.
[35] D.F. Lázaro, M.A.S. Pavlou, T.F. Outeiro, Cellular models as tools for the study of the role of alpha-synuclein in Parkinson's disease, Exp. Neurol. 298 (2017) 162–171.
[36] A.M. Poehler, W. Xiang, P. Spitzer, V.E.L. May, H. Meixner, E. Rockenstein, O. Chutna, T.F. Outeiro, J. Winkler, E. Masliah, J. Klucken, Autophagy modulates SNCA/α-synuclein release, thereby generating a hostile microenvironment, Autophagy 10 (2014) 2171–2192.
[38] C.R. Bodner, C.M. Dobson, A. Bax, Multiple tight phospholipid-binding modes of alpha-synuclein revealed by solution NMR spectroscopy, J. Mol. Biol. 390 (2009) 775–790.
[39] F. Chiti, C.M. Dobson, Protein misfolding, functional amyloid, and human disease, Annu. Rev. Biochem. 75 (2006) 333–366.
[40] M.M. Dedmon, K. Lindorff-Larsen, J. Christodoulou, M. Vendruscolo, C.M. Dobson, Mapping long-range interactions in alpha-synuclein using spin-label NMR and ensemble molecular dynamics simulations, J. Am. Chem. Soc. 127 (2005) 476–477.
[41] B. Fauvet, M.K. Mbefo, M.-B. Fares, C. Desobry, S. Michael, M.T. Ardah, E. Tsika, P. Coune, M. Prudent, N. Lion, D. Eliezer, D.J. Moore, B. Schneider, P. Aebischer, O.M. El-Agnaf, E. Masliah, H.A. Lashuel, α-Synuclein in central nervous system and from erythrocytes, mammalian cells, and *Escherichia coli* exists predominantly as disordered monomer, J. Biol. Chem. 287 (2012) 15345–15364.
[42] T. Bartels, J.G. Choi, D.J. Selkoe, W. Hospital, A-Synuclein occurs physiologically as a helically folded tetramer that resists aggregation, Nature 477 (2012) 107–110.
[43] E. Lindersson, D. Lundvig, C. Petersen, P. Madsen, J.R. Nyengaard, P. Højrup, T. Moos, D. Otzen, W. Gai, P.C. Blumbergs, P.H. Jensen, P25a Stimulates a-Synuclein aggregation and Is Co-localized with Aggregated a-Synuclein in a-Synucleinopathies *, J. Biol. Chem. 280 (2005) 5703–5715.
[44] V. Dias, E. Junn, M.M. Mouradian, The role of oxidative stress in Parkinson's disease, J. Park. Dis. 3 (2014) 461–491.
[45] A.A. Valiente-Gabioud, V. Torres-Monserrat, L. Molina-Rubino, A. Binolfi, C. Griesinger, C.O. Fernández, Structural basis behind the interaction of Zn2+ with the protein α-synuclein and the Aβ peptide: a comparative analysis, J. Inorg. Biochem. 117 (2012) 334–341.
[46] B. Wolozin, N. Golts, Iron and Parkinson ' s disease, Neurosci 60153 (2002) 22–32.
[47] F. Opazo, A. Krenz, S. Heermann, J.B. Schulz, B.H. Falkenburger, Accumulation and clearance of α-synuclein aggregates demonstrated by time-lapse imaging, J. Neurochem. 106 (2008) 529–540.
[48] C.C. Rospigliosi, S. McClendon, A.W. Schmid, T.F. Ramlall, P. Barré, H.A. Lashuel, D. Eliezer, E46K Parkinson's-linked mutation enhances C-terminal-to-N-terminal contacts in alpha-synuclein, J. Mol. Biol. 388 (2009) 1022–1032.
[49] D. Bhattacharyya, R. Kumar, S. Mehra, A. Ghosh, S.K. Maji, A. Bhunia, Multitude NMR studies of α-synuclein familial mutants: probing their differential aggregation propensities, Chem. Commun. 54 (2018) 3605–3608.
[50] K. Nakamura, V.M. Nemani, E.K. Wallender, K. Kaehlcke, M. Ott, R.H. Edwards, Optical reporters for the conformation of alpha-synuclein reveal a specific interaction with mitochondria, J. Neurosci. 28 (2008) 12305–12317.
[51] C.W. Bertoncini, Y.-S. Jung, C.O. Fernandez, W. Hoyer, C. Griesinger, T.M. Jovin, M. Zweckstetter, From the cover: release of long-range tertiary interactions potentiates aggregation of natively unstructured -synuclein, Proc. Natl. Acad. Sci. 102 (2005) 1430–1435.
[52] M. Sharma, T.C. Su, Definition of a molecular pathway mediating a-Synuclein, J. Neurosci. 35 (2015) 5221–5232.
[53] J. Burre, M. Sharma, T.C. Sudhof, Definition of a molecular pathway mediating -Synuclein neurotoxicity, J. Neurosci. 35 (2015) 5221–5232.
[54] C. Galvagnion, J.W.P. Brown, M.M. Ouberai, P. Flagmeier, M. Vendruscolo, A.K. Buell, E. Sparr, C.M. Dobson, Chemical properties of lipids strongly affect the kinetics of the membrane-induced aggregation of α-synuclein, Proc. Natl. Acad. Sci. 113 (2016) 7065–7070.
[55] M. Zhu, J. Li, A.L. Fink, The association of alpha-synuclein with membranes affects bilayer structure, stability, and fibril formation, J. Biol. Chem. 278 (2003) 40186–40197.
[56] R. Sharon, I. Bar-Joseph, M.P. Frosch, D.M. Walsh, J.A. Hamilton, D.J. Selkoe, The formation of highly soluble oligomers of alpha-synuclein is regulated by fatty acids and enhanced in Parkinson's disease, Neuron 37 (2003) 583–595.
[57] R.L. Croke, C.O. Sallum, E. Watson, E.D. Watt, A.T. Alexandrescu, Hydrogen exchange of monomeric alpha-synuclein shows unfolded structure persists at physiological temperature and is independent of molecular crowding in *Escherichia coli*, Protein Sci. 17 (2008) 1434–1445.
[58] C. Gomes-Trolin, I. Nygren, S.-M. Aquilonius, H. Askmark, Increased red blood cell polyamines in ALS and Parkinson's disease, Exp. Neurol. 177 (2002) 515–520.
[59] M.C. Miotto, A.A. Valiente-Gabioud, G. Rossetti, M. Zweckstetter, P. Carloni, P. Selenko, C. Griesinger, A. Binolfi, C.O. Fernández, Copper binding to the N-terminally acetylated, naturally occurring form of alpha-Synuclein induces local helical folding, J. Am. Chem. Soc. 137 (2015) 6444–6447.
[60] A. Villar-Piqué, T. Lopes da Fonseca, R. Sant'Anna, É. Szegö, L. Fonseca-Ornelas, R. Pinho, A. Carija, E. Gerhardt, C. Masaracchia, E. Abad Gonzalez, G. Rossetti, P. Carloni, C.O. Fernández, D. Foguel, I. Milosevic, M. Zweckstetter, S. Ventura, T.F. Outeiro, Environmental and genetic factors support the dissociation between α-synuclein aggregation and toxicity, Proc. Natl. Acad. Sci. U. S. A. 113 (2016) E6506–E6515.
[61] Y. Lu, M. Prudent, B. Fauvet, H.A. Lashuel, H.H. Girault, Phosphorylation of a-synuclein at Y125 and S129 alters its metal binding properties: implications for understanding the role of a-synuclein in the pathogenesis of Parkinson's disease and related disorders, ACS Chem. Neurosci. 2 (2011) 667–675.
[62] W. Li, N. West, E. Colla, O. Pletnikova, J.C. Troncoso, L. Marsh, T.M. Dawson, P. Jäkälä, T. Hartmann, D.L. Price, M.K. Lee, Aggregation promoting C-terminal truncation of alpha-synuclein is a normal cellular process and is enhanced by the familial Parkinson's disease-linked mutations, Proc. Natl. Acad. Sci. U. S. A. 102 (2005) 2162–2167.
[63] K. Beyer, A. Ariza, Alpha-Synuclein posttranslational modification and alternative splicing as a trigger for Neurodegeneration, Mol. Neurobiol. (2012), https://doi.org/10.1007/s12035-012-8330-5.
[64] M. Johnson, M.A. Geeves, D.P. Mulvihill, Production of amino-terminally acetylated recombinant proteins in E. Coli, Methods Mol. Biol. (2015), https://doi.org/10.1007/978-1-62703-305-3.
[65] P. Schanda, E. Kupče, B. Brutscher, SOFAST-HMQC experiments for recording two-dimensional deteronuclear correlation spectra of proteins within a few seconds, J. Biomol. NMR 33 (2005) 199–211.
[66] A.S. Maltsev, J. Ying, A. Bax, Impact of N-terminal acetylation of α-Synuclein on its random coil and lipid binding properties, Biochemistry 51 (2012) 5004–5013.
[67] G.R. Lamberto, A. Binolfi, M.L. Orcellet, C.W. Bertoncini, M. Zweckstetter, C. Griesinger, C.O. Fernández, Structural and mechanistic basis behind the inhibitory interaction of PcTS on alpha-synuclein amyloid fibril formation, Proc. Natl. Acad. Sci. U. S. A. 106 (2009) 21057–21062.
[68] N.A. Farrow, O. Zhang, J.D. Forman-Kay, L.E. Kay, Comparison of the backbone dynamics of a folded and an unfolded SH3 domain existing in equilibrium in aqueous buffer, Biochemistry 34 (1995) 868–878.
[69] A. Binolfi, C.O. Fernández, M.P. Sica, J.M. Delfino, J. Santos, Recognition between a short unstructured peptide and a partially folded fragment leads to the thioredoxin fold sharing native-like dynamics, Proteins Struct. Funct. Bioinforma. 80 (2012) 1448–1464.
[70] L. Serrano, Comparison between the phi distribution of the amino acids in the protein database and NMR data indicates that amino acids have various phi propensities in the random coil conformation, J. Mol. Biol. 254 (1995) 322–333.